1986ApJ...305..714H

THE ASTROPHYSICAL JOURNAL, 305:714–720, 1986 June 15
© 1986. The American Astronomical Society. All rights reserved. Printed in U.S.A.

FORMATION OF OB CLUSTERS: RADIATION-DRIVEN IMPLOSION?

PAUL T. P. HO[1]
Harvard-Smithsonian Center for Astrophysics
RICHARD I. KLEIN
University of California, Lawrence Livermore National Laboratory, and Berkeley Department of Astronomy
AND
AUBREY D. HASCHICK
Haystack Observatory
Received 1985 September 10; accepted 1985 December 6

ABSTRACT

New high dynamic range (1000–2000) radio continuum maps were obtained for two regions of vigorous star formation, G10.6−0.4 and W33. The morphology of an extended low-level ionized emission component is successfully defined. Ionized gas due to an earlier epoch of star formation appears to flow around and fill in between dense neutral condensations. Bright rims are found facing toward the central continuum core where the most recent episode of star formation is taking place. This supports a model where radiation-driven ionization shock fronts from first-generation OB stars lead to the efficient implosion of nearby neutral condensations and the formation of second generation stars.

Subject headings: clusters: open — stars: formation

I. INTRODUCTION

Recent radio continuum experiments on the VLA (Ho and Haschick 1981; Haschick and Ho 1983; Dreher *et al.* 1984) have demonstrated the presence of complex small-scale structures within compact H II regions. From the association of some of these continuum knots with OH masers (thought to reside in neutral circumstellar shells; see Reid *et al.* 1980), as well as luminosity arguments, it seems reasonable that a number of exciting sources are present in each of these compact H II regions. The small sizes ($\lesssim 0.1$ pc) of the individual knots suggest that a cluster of OB stars has recently formed together in a burst over a very short period of time ($\sim 10^4$ yr).

For the smallest knots observed (e.g., W49; Dreher *et al.* 1984), the apparent dynamical time scales ($\sim 10^3$ yr) seem uncomfortably short compared to free-fall or pre–main-sequence evolution time scale. The apparent youth of these regions and the synchronization of their arrival times on the main sequence seem difficult to explain. Two suggestions have been made recently that may help explain this behavior. First, observations of the compact H II region G10.6−0.4 reveal infall of material at ~ 5 km s^{-1} toward the central stars (Ho and Haschick 1986). The deduced pressure of the accretion flow seems sufficient for restraining the expansion of the H II regions. Hence, the true dynamical time scales are probably longer. Other evidences of infall are the apparent redshifted motions of OH masers with respect to the H II regions (see Garay, Reid, and Moran 1985). Second, Klein, Sandford, and Whitaker (1983) suggest that radiation-driven shock waves originating from the ionization-shock interaction of UV radiation from an earlier generation of OB stars can implode ambient cloud condensations. Compression by a factor of $\gtrsim 200$ can be achieved in 3×10^4 yr, to be followed by collapse within 6×10^4 yr. This mechanism suggests a means to synchronize the formation of multiple massive stars.

In this paper, we report a high-sensitivity continuum study of the low-level emission in two well-studied regions, G10.6−0.4 and W33. The goals are to detect the presence and define the morphology of earlier generations of star formation. We find that the most recent burst of star formation seems, indeed, to occupy a central location.

II. OBSERVATIONS

The continuum data were obtained with the Very Large Array (VLA) of the National Radio Astronomy Observatory[2] near Socorro, New Mexico, on 1984 June 12. The array was in the C-configuration, with physical separations of the antennas ranging from 63 m to 3.4 km. We observed the two fields, G10.6−0.4 and W33, during an 8 hr track alternating between $\lambda = 6$ cm and 20 cm. The phase centers were R.A.(1950) = $18^h07^m30^s.68$, decl.(1950) = $-19°56'28''.4$ and R.A.(1950) = $18^h11^m18^s.50$, decl.(1950) = $-17°56'40''.3$. Our primary flux calibrator was 3C 286, with the assumed fluxes of 14.5 (7.41) Jy at 1.465 (4.885) GHz during the epoch of our observations. Our phase calibrator was 1730−130 (NRAO 530) at $\lambda = 6$ cm and 1741−038 at $\lambda = 20$ cm, with measured fluxes of 5.87 ± 0.02 and 1.75 ± 0.02 Jy, respectively. All of our maps have been CLEANed (Clark 1980) and self-calibrated (Schwab 1980). The absolute positional accuracy of our maps is on the order of $0''.1$. The achieved rms noise was limited by dynamic range to ~ 1 mJy. We have not applied primary beam correction since the structures of interest are small compared to the antenna beam. However, bandwidth smearing with the full 50 MHz window resulted in the loss of sensitivity of $\sim 50\%$ at $\sim 9'$ from field center. Because of missing short spacings, structures larger than $3'$ ($80''$) are significantly resolved at 20 cm (6 cm) by the interferometer.

Our continuum maps are presented in Figures 1 and 2. A dynamic range (peak flux to rms flux) of 1000–2000 was achieved for all the maps. The most interesting result is that in

[1] Alfred P. Sloan Foundation Fellow.

[2] The National Radio Astronomy Observatory is operated by Associated Universities, Inc., under contract to the National Science Foundation.

© American Astronomical Society • Provided by the NASA Astrophysics Data System

1986ApJ...305..714H

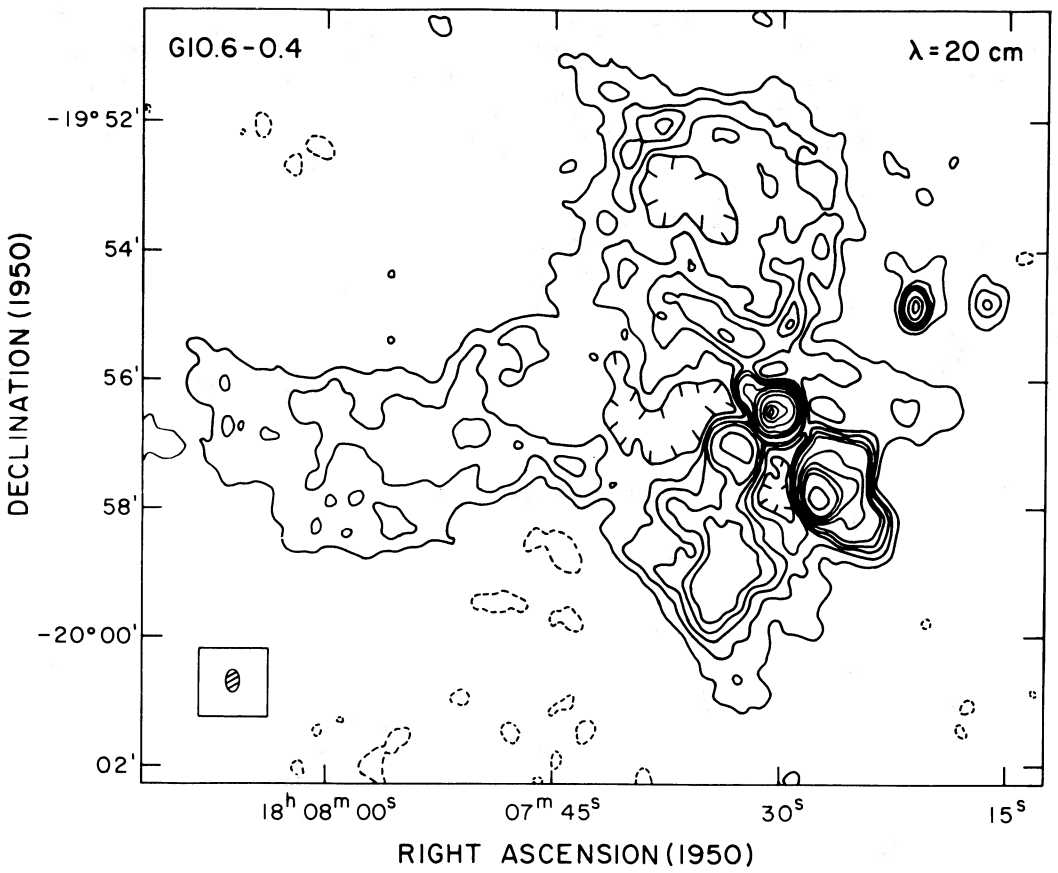

FIG. 1*a*

FIG. 1.—(*a*) 20 cm continuum map of G10.6−0.4. Contour levels are −8, −4, 4, 8, 12, 16, 20, 40, 60, 80, 100, 200, 400, 500, 600 mJy per beam. Peak flux is 660 mJy per beam. Synthesized beam is 20.3″ × 12.9″ and is indicated as a hatched ellipse. Brightness temperature is 0.30 K mJy^{-1}. The well-studied compact core is located in the center of an extended complex. Note a number of "holes" in the continuum distribution. In the north, a "hole" defines a ringlike structure. In the south, the "holes" are located adjacent to steep boundaries of emission knots. (*b*) 6 cm continuum map of G10.6−0.4. Contour levels are −10, −5, −2.5, 2.5, 5, 10, 20, 40, 80, 160, 320, 640 mJy per beam. Peak flux is 1.26 Jy per beam. Synthesized beam is 6.8″ × 3.6″ and is indicated. Brightness temperature is 3.1 K mJy^{-1}. Of interest in this map is the smoothness of the extended structures that are mostly resolved. Only the central core reveals a "clumpy" appearance. We interpret this as indicating that the core is younger and likely to be composed of a cluster of OB stars.

both cases, the central compact core is embedded in a weaker and extended complex. This extended structure detected at 20 cm with ∼20″ resolution appears smooth. Almost certainly this extended emission is optically thin and thermal with a flat spectral index. Thus the failure to detect the bulk of the extended structures at 6 cm with ∼7″ resolution is an indication of the smoothness of the emission and the lack of small-scale structures. The compact core, on the other hand, shows an abundance of clumpy structures at 6 cm under higher resolution, consistent with earlier results (Ho and Haschick 1981).

Parts of the extended structures show bright-rim type appearances. This is suggested by the steepness of the contours in the 20 cm maps and the detection of the "rims" in the 6 cm maps. The orientations of these bright rims are interesting. In both G10.6−0.4 and W33, the bright rims tend to face inward, although not always perfectly toward the core.

III. DISCUSSION

a) Comparison with Earlier Results

For the compact cores, the increased dynamic range of the present maps has revealed additional weak features heretofore undetected. In the case of G10.6−0.4 (Fig. 1*b*), the extensions *I* and *J* at the 10 mJy level to the northeast and south and the compact condensations *K* and *L* were missed in previous studies. In the case of W33 (Fig. 2*b*), the extensions *H* and *I* at the 20 mJy level to the southeast and northwest, and the new condensation *J*, are below the noise level of previous maps (Haschick and Ho 1983; Wynn-Williams, Beichman, and Downes 1981). From the detected flux densities, ∼100–200 mJy, we conclude that these new low-level emissions may be due to B0 and lower mass stars that are apparently part of the central cluster.

For the extended emissions, we estimate that we are missing on the order of $\gtrsim$20% of the single-dish flux, probably in very extended (>3′) structures. Our new results provide better definition of the morphology because of the better dynamic range and the deconvolution of the beam pattern. This latter effect can be important in single-dish maps of extended structures. Altenhoff *et al.* (1978) with an angular resolution of 2′.6 report the presence of the weaker complexes G10.76−0.47 and G10.76−0.41. We find that these weaker extensions together define the arclike structure northeast of G10.6−0.4 (Fig. 1*a*). Altenhoff *et al.* also detect the W33 complex (G12.8−0.2), as did Goss, Matthews, and Winnberg (1978) and Bieging,

© American Astronomical Society • Provided by the NASA Astrophysics Data System

1986ApJ...305..714H

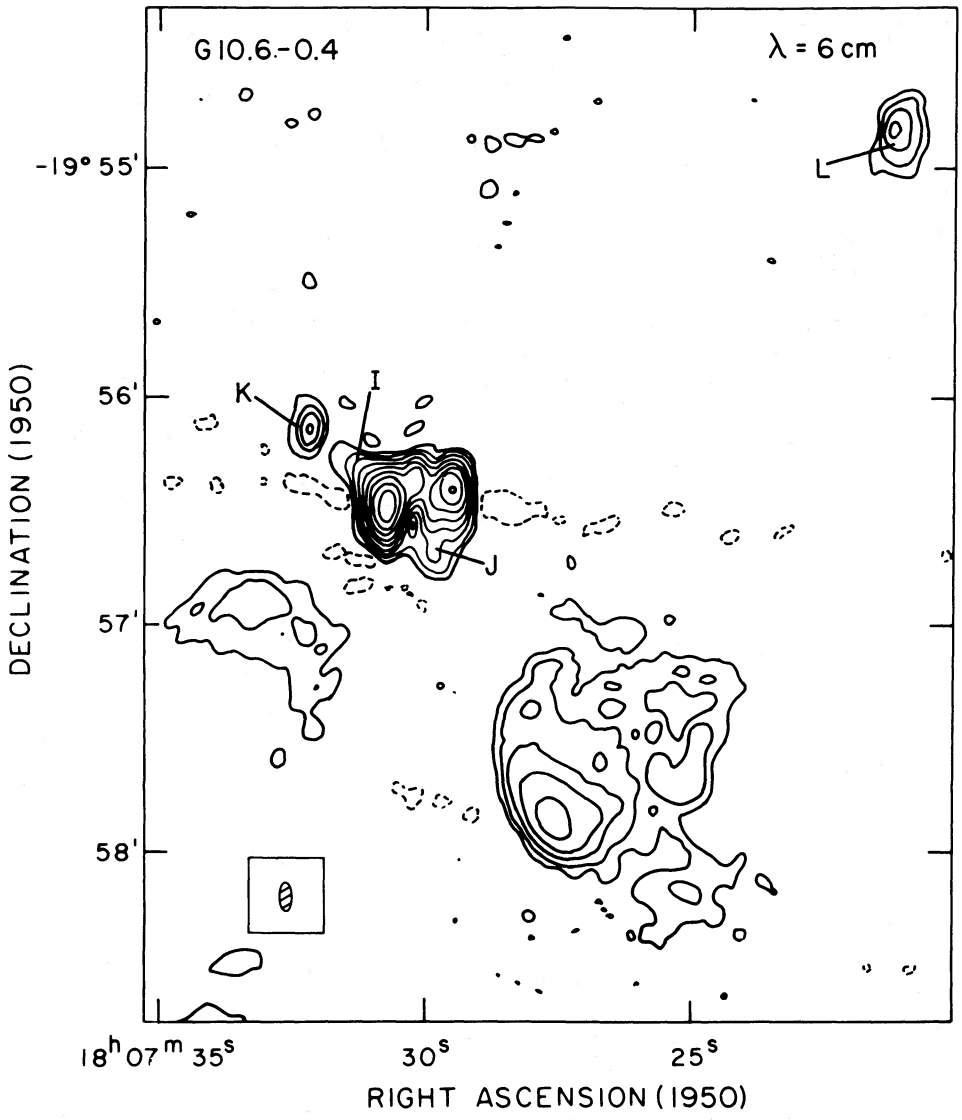

FIG. 1*b*

Pankonin, and Smith (1978) with ~1'.5 resolution. With 20″ resolution, we find that the weak extended structure on the western side of W33 appears to be a single complex, even though the single-dish studies have suggested that there may be individual condensations. Finally, bright rimlike structures are found, which have important implications on any proposed model of these regions.

b) The Relation between the Continuum Emission and Molecular Cloud Structures

We are interested in examining the possibility that earlier generations of OB stars could have triggered the formation of the central core. In this regard, we examine the juxtaposition of the ionized material with respect to the neutral cloud matter. Figure 3 shows an overlay of the 20 cm maps (this paper) with NH_3 maps of the molecular clouds (Ho *et al.* 1986; Haschick and Ho 1983). It should be noted that such comparisons can be misleading because the data are aways two-dimensional projections. Nevertheless, the compact cores are clearly well centered with molecular material, while the extended structures are more on the periphery.

In the case of G10.6−0.4, the arclike continuum structure to the northeast is found just outside the ridge of NH_3 condensations. CO studies (Ho *et al.* 1986) show that even low-density neutral gas is absent to the northeast of the continuum arc. Hence the extended arc is at the boundary and is most likely impacting against the molecular cloud. The most intense continuum emission arises from the core of one of the NH_3 condensations. The bright rims facing this central core are probably D-type ionization fronts at the edge of the core. Significantly, the ionization assumes a more open configuration to the south, seemingly flowing and expanding in between two NH_3 condensations. This is reminiscent of the champagne model (Tenorio-Tagle 1979; Bodenheimer, Tenorio-Tagle, and Yorke 1979; Icke, Gatley, and Israel 1980), where the originally confined H II region bursts through the boundary of a molecular cloud. To the northwest, the continuum emission again skirts around an NH_3 condensation, possibly causing the star formation behind this front. Since the sound crossing time is $\gtrsim 10^6$ yr across the extended continuum complex, the clumpy

© American Astronomical Society • Provided by the NASA Astrophysics Data System

1986ApJ...305..714H

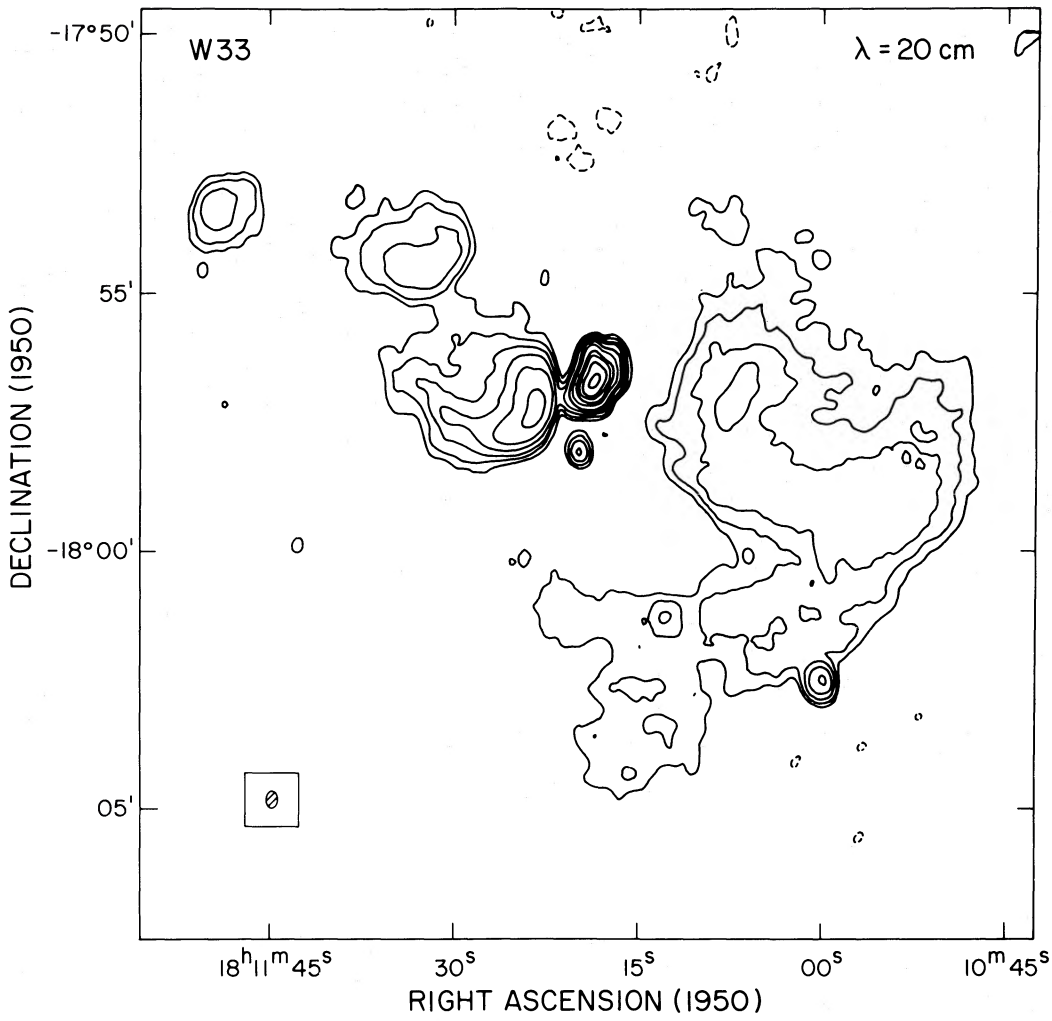

FIG. 2a

FIG. 2.—(*a*) 20 cm continuum map of W33. Contour levels are −16, −8, 8, 16, 32, 64, 128, 300, 600, 1000, 1500, 2500 mJy per beam. Peak flux is 2.76 Jy per beam. Synthesized beam is 20.9″ × 13.5″ and is indicated as a hatched ellipse. Brightness temperature is 0.28 K mJy^{-1}. As in the case of G10.6−0.4, a central core is surrounded by weaker extended emission. The complex immediately to the east of the central core shows a steep boundary on its western front. (*b*) 6 cm continuum map of W33. Contour levels are −10, −5, 5, 10, 20, 40, 80, 160, 320, 640, 1280 mJy per beam. Peak flux is 1.94 Jy per beam. Synthesized beam is 6.5″ × 3.9″ and is indicated. Brightness temperature is 3.0 K mJy^{-1}. The morphology at 6 cm is again similar to that of G10.6−0.4. The extended structure is smooth, while the central core is clumpy. A central young cluster of OB stars is again implied.

and more intense structures in the southwest probably represent a later episode of star formation as compared to the arc in the northeast.

In the case of W33, the extended continuum source immediately east of the compact core (source *h* in the notation of Bieging, Pankonin, and Smith 1978) is seen to be nestled in a bend in the NH_3 structure. The bright rimlike structure faces the NH_3 cloud and the central compact continuum core. The extended complex to the west (sources *a–f* in the notation of Bieging, Pankonin, and Smith 1978) is seen to wrap around the NH_3 condensation on the southwestern side. However, the correspondence is not perfect, since the extended source 3′ to the northeast appears embedded in the molecular cloud. It is possible that this is due to project effects.

The overall impression is that the extended continuum emission represents ionization fronts driven into the molecular clouds by an earlier generation of O stars. It is not certain that the earlier episode of star formation occurred at the cloud boundary. It is more likely that the ionization from these stars has defined the new cloud boundaries. A most notable point is that wherever the extended continuum emission encounters dense cloud condensations, the ionization appears to "flow" around them. Finally, the extended structures appear to be driven by relatively lower mass stars, O7 or later (see Bieging, Pankonin, and Smith 1978). The concentration of the more massive stars toward the center appears to be an important clue.

c) Radiation-driven Implosion

The problem of secondary star formation has been recently reviewed by Klein, Whitaker, and Sandford (1985). It has been suggested that the ionization and shock fronts generated by OB stars can lead to subsequent second generation star formation in nearby molecular material (see Blaauw 1964; Kossacki

© American Astronomical Society • Provided by the NASA Astrophysics Data System

1986ApJ...305..714H

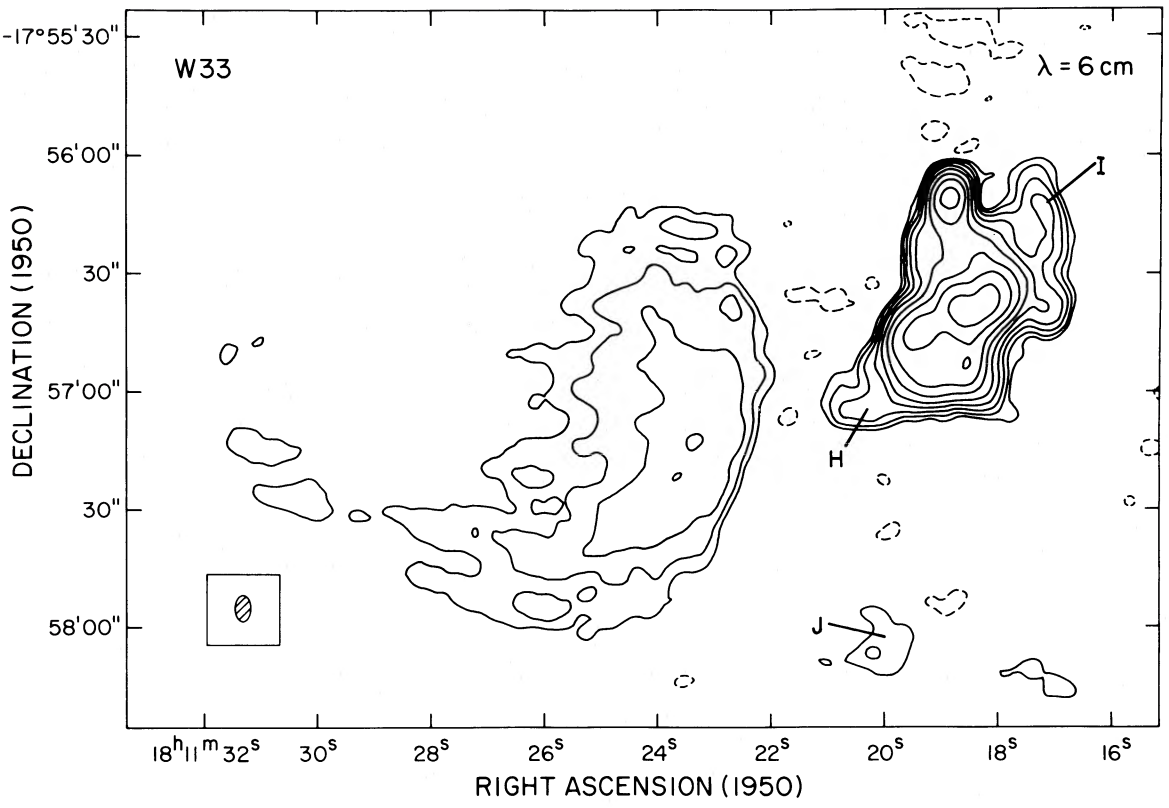

FIG. 2*b*

1968; Elmegreen and Lada 1977). Two-dimensional radiation-hydrodynamical numerical calculations (Klein, Sandford, and Whitaker 1983; 1986) improve upon the analytic solutions of Elmegreen and Lada by showing that the radiation-driven shock waves from O stars can efficiently compress neutral cloud condensations on a time scale of $\sim 10^4$ yr. The photoionization and the resultant ablation of the surface layer of a cloud condensation propagate convergent shock waves into the neutral material. The large compressions achieved can drive the cloud into gravitational collapse over short time scales. For this mechanism to work, the first-generation stars cannot be too luminous ($10^4 < L_* < 10^5\ L_\odot$), and there must be substantial mass in the neutral cloudlet. Otherwise, the condensations cannot survive the ionization and evaporation.

Our new maps of G10.6−0.4 and W33 give support to this radiation-driven implosion model. First, the morphology of the continuum emission suggests that ionized material is indeed flowing around neutral obstructions. Such flows will give rise to multidimensional convergent shocks that result in far greater compression than would be possible for planar fronts. Second, the presence of the bright rims near the central core supports the notion that ionization fronts are being driven into the neutral material. The presence of neutral matter is indicated by the NH_3 emission (Fig. 3). Higher angular resolution studies show that the central continuum core is embedded in a rapidly rotating NH_3 condensation (Ho and Haschick 1986). The observed gap between the bright rims and the central core (Figs. 1*b*, 2*b*) is consistent with the presence of an intervening neutral cloud. That compression and star formation result from external influences seems likely. Finally, we also find that the older stars (by virtue of their larger H II regions and hence longer dynamical time scales) are relatively lower mass stars, O7 or later. This is consistent with the implosion model where more massive first-generation stars would have been much more effective in destroying the neutral condensations.

There are a few problems still to be pursued in these studies. The implosion model suggests a cutoff in lower mass stars by virtue of the failure of smaller condensations to survive against evaporation. The data are consistent with this since stars less massive than B0 are underabundant by comparing the radio continuum and far-infrared luminosities (Ho and Haschick 1981; Haschick and Ho 1983). However, this conclusion is uncertain because of the dependence on the initial mass function, the nonuniqueness in identifying the spectral types, and possible dynamic range and short-spacing effects both in the radio and infrared data. There is also a problem with the material ablated from the neutral condensations by the surrounding first-generation stars. Significant amounts of the original mass can be lost through this process (Klein, Sandford, and Whitaker 1985). This material has not been seen since the total ionized matter apparently carries only a small fraction of the total mass in the region. At the measured electron densities of greater than 10^2 cm^{-3}, the recombination time is less than 10^3 yr. Hence, this ionized ablated material will recombine as it moves away from the source of ionization. Actually detecting and measuring the properties of this component will be crucial for the model. The dynamics of the detected ionized gas will be an important key in proving that ionization fronts are being driven toward the center. Higher angular resolution and more sensitive studies of the recombination lines detected by Bieging, Pankonin, and Smith (1978)

© American Astronomical Society • Provided by the NASA Astrophysics Data System

1986ApJ...305..714H

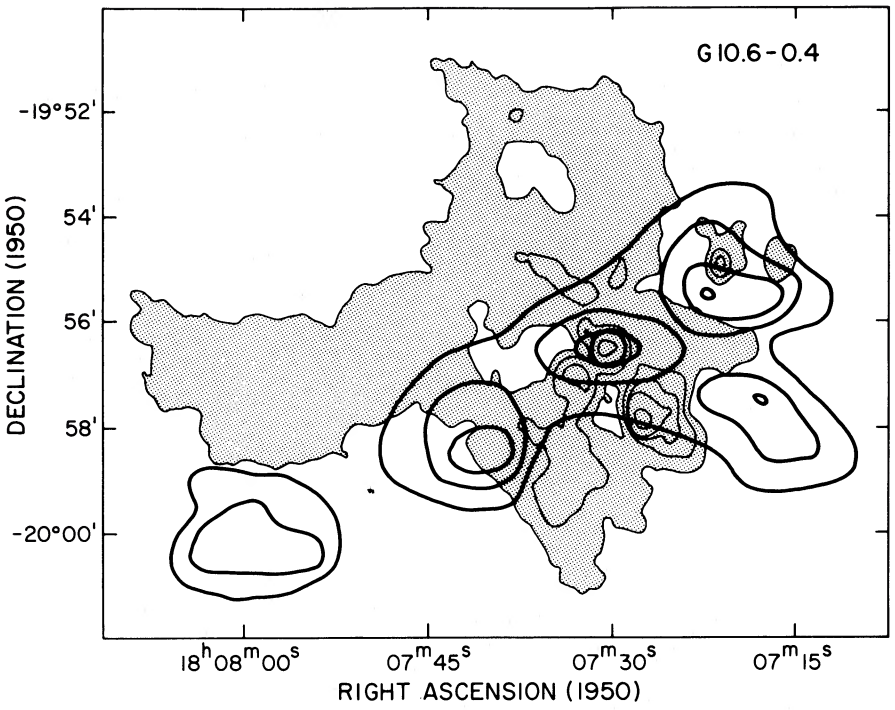

FIG. 3*a*

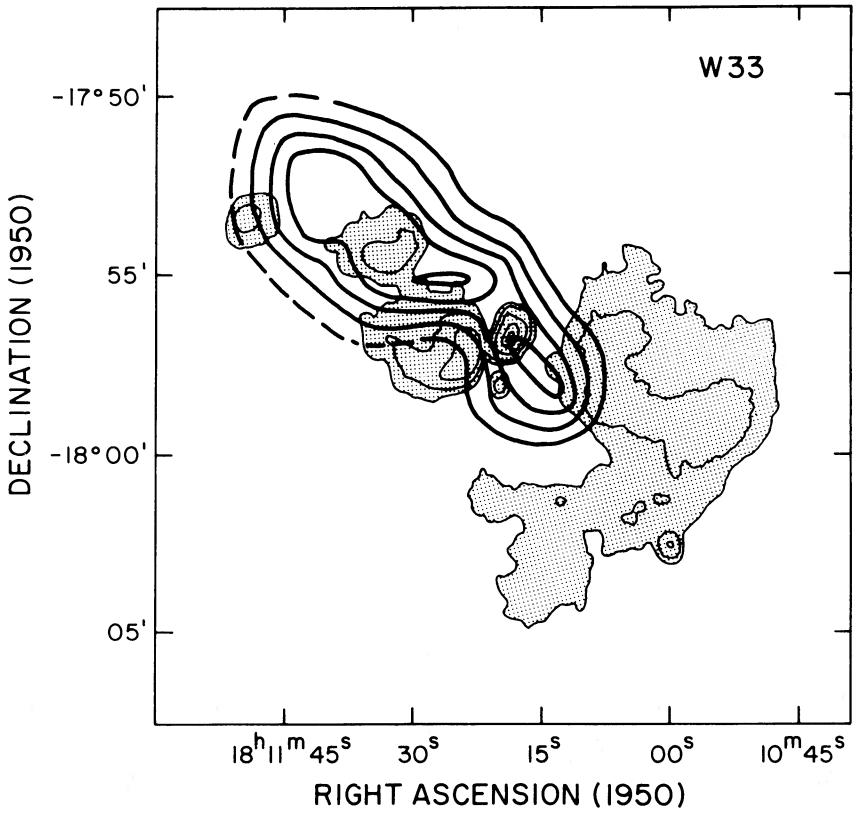

FIG. 3*b*

FIG. 3.—(*a*) Superposition of 20 cm continuum map (*stippled*) of G10.6−0.4 with 1 cm NH_3 line emission map from Ho *et al.* (1986). Note the location of the continuum arc on the northeast side of the ridge of NH_3 condensations. The region northeast of this continuum arc shows almost no neutral material. Toward the south, note the apparent escape of ionized material in the bays between the neutral condensations. (*b*) Superposition of 20 cm map of W33 with 1 cm NH_3 line emission map from Haschick and Ho (1983). Note the bright rimlike continuum structure, east of the central core. Steep contours coincide with the boundary of the NH_3 cloud. Similarly, the extended complex to the southwest seems to wrap around the neutral emission region. However, there is the extended continuum emission 3′ to the northeast that appears embedded in molecular material. This may be due to projection.

© American Astronomical Society • Provided by the NASA Astrophysics Data System

1986ApJ...305..714H

and a comparison with the molecular material should reveal signs of interaction. Studies in these directions are in progress.

Radio Astronomy at Haystack Observatory of the Northeast Radio Corporation is supported by the National Science Foundation under grant AST 82-10570. P. T. P. H. is supported in part by the National Science Foundation under grant AST 85-09907. We thank John Dreher for helpful suggestions on the manuscript.

REFERENCES

Altenhoff, W. J., Downes, D., Pauls, T., and Schraml, J. 1978, *Astr. Ap. Suppl.*, **35**, 23.
Bieging, J. H., Pankonin, V., and Smith, L. F. 1978, *Astr. Ap.*, **64**, 341.
Blaauw, A. 1964, *Ann. Rev. Astr. Ap.*, **2**, 213.
Bodenheimer, P., Tenorio-Tagle, G., and Yorke, H. W. 1979, *Ap. J.*, **233**, 95.
Clark, B. G. 1980, *Astr. Ap.*, **89**, 377.
Dreher, J. W., Johnston, K. J., Welch, W. J., and Walker, R. C. 1984, *Ap. J.*, **283**, 632.
Elmegreen B. G., and Lada, C. J. 1977, *Ap. J.*, **214**, 725.
Garay, G., Reid, M. J., and Moran, J. M. 1985, *Ap. J.*, **289**, 681.
Goss, W. M., Matthews, H. E., and Winnberg, A. 1978, *Astr. Ap.*, **65**, 307.
Haschick, A. D., and Ho, P. T. P. 1983, *Ap. J.*, **267**, 638.
Ho, P. T. P., and Haschick, A. D. 1981, *Ap. J.*, **248**, 622.
———. 1986, *Ap. J.*, **304**, 501.
Ho, P. T. P., Haschick, A. D., Snell, R. L., and Klein, R. I. 1986, in preparation.
Icke, V., Gatley, I., and Israel, F. P. 1980, *Ap. J.*, **236**, 838.
Klein, R. I., Sandford M. T., II, and Whitaker, R. W., 1983, *Ap. J.* (*Letters*), **271**, L69.
———. 1986, in preparation.
Klein, R. I., Whitaker, R. W., and Sandford, M. T., II. 1985, in *Proc. 2d Protostars and Planets Conf.* ed. D. C. Black and M. S. Matthews (Tucson: University of Arizona Press), p. 340.
Kossacki, K. 1968, *Acta Astr.*, **18**, 221.
Reid, M. J., Haschick, A. D., Burke, B. F., Moran, J. M., Johnston, K. J., and Swenson, G. W., Jr. 1980, *Ap. J.*, **239**, 89.
Schwab, F. 1980, *Proc. SPIE*, **231**, 18.
Tenorio-Tagle, G. 1979, *Astr. Ap.*, **71**, 59.
Wynn-Williams, C. G., Beichman, C. A., and Downes, D. 1981, *A.J.*, **86**, 565.

AUBREY D. HASCHICK: Haystack Observatory, NEROC, Westford, MA 01886

PAUL T. P. HO: Department of Astronomy, Harvard-Smithsonian Center for Astrophysics, 60 Garden Street, Cambridge, MA 02138

RICHARD I. KLEIN: Lawrence Livermore National Laboratory, L-18 University of California, P. O. Box 808, Livermore, CA 94550

© American Astronomical Society • Provided by the NASA Astrophysics Data System